Pharmaceutical Research, Vol. 22, No. 3, March 2005 (© 2005)
DOI: 10.1007/s11095-004-1870-2

Research Paper

Compartmental Modeling of Transdermal Iontophoretic Transport II: *In Vivo* Model Derivation and Application

Akhmad Kharis Nugroho,[1,2] Oscar Della-Pasqua,[3] Meindert Danhof,[3] and Joke A. Bouwstra[1,4]

Received July 18, 2004; accepted December 9, 2004

Purpose. This study was aimed to develop a family of compartmental models to describe in a strictly quantitative manner the transdermal iontophoretic transport of drugs *in vivo*. The new models are based on previously proposed compartmental models for the transport *in vitro*.
Methods. The novel *in vivo* model considers two separate models to describe the input into the systemic circulation: a) constant input and b) time-variant input. Analogous to the *in vitro* models, the *in vivo* models contain four parameters: 1) kinetic lag time (t_L), 2) steady-state flux during iontophoresis (J_{ss}), 3) skin release rate constant (K_R), and 4) passive flux in the post-iontophoretic period (J_{pas}). The elimination from the systemic circulation is described by a) the one-compartment and b) the two-compartment pharmacokinetic models. The models were applied to characterize the observed plasma concentration vs. time data following single-dose iontophoretic delivery of growth hormone-releasing factor (GRF) and R-apomorphine. Moreover, the models were also used to simulate the observed plasma concentration *vs.* time profiles following a two-dose transdermal iontophoretic administration of alniditan.
Results. The time-variant input models were superior to the constant input models and appropriately converged to the observed data of GRF and R-apomorphine allowing the estimation of J_{ss}, K_R, and J_{pas}. In most cases, the values of t_L were negligible. The estimated J_{ss} and the *in vivo* flux profiles of GRF and R-apomorphine were similar to those obtained using the deconvolution method. The two-dose iontophoretic transport of alniditan was properly simulated using the proposed time-variant input model indicating the utility of the model to predict and to simulate the drug transport by a multiple-dose iontophoresis. Moreover, the use of the compartmental modeling approach to derive an *in vitro–in vivo* correlation for R-apomorphine was demonstrated. This approach was also used to identify the optimum *in vitro* model that closely mimics the *in vivo* iontophoretic transport of R-apomorphine.
Conclusions. The developed *in vivo* models demonstrate their consistency and capability to describe the *in vivo* iontophoretic drug transport. This compartmental modeling approach provides a scientific basis to examine *in vitro–in vivo* correlations of drug transport by iontophoresis.

KEY WORDS: alniditan; GRF; R-apomorphine; skin release rate constant; steady-state flux.

INTRODUCTION

Recently (1), we have proposed a family of compartmental models to describe iontophoretic drug transport *in vitro*. The model was able to describe the iontophoretic transport of apomorphine *per se* and after surfactant pretreatment (2). The model parameter values describing the transport (i.e., J_{ss}) were very close to those obtained with the standard diffusion lag time method, supporting the validity of this approach as an alternative method to handle iontophoretic diffusion *in vitro* (1).

[1] Division of Drug Delivery Technology, Leiden/Amsterdam Center for Drug Research, 2300 RA Leiden, The Netherlands.
[2] Faculty of Pharmacy, Gadjah Mada University, Yogyakarta 55281, Indonesia.
[3] Division of Pharmacology, Leiden/Amsterdam Center for Drug Research, 2300 RA Leiden, The Netherlands.
[4] To whom correspondence should be addressed. (e-mail: bouwstra@chem.leidenuniv.nl)

ABBREVIATIONS: α and β, micro constants obtained during integration/Laplace transformation; A_T, the amount of drug presence in the central compartment at current removal; A_{2T}, the amount of drug presence in the peripheral compartment at current removal; A(t), drug amount in plasma at time t; Cp(t), drug concentration in the central compartment (plasma) at time t; DHS, dermatomed human skin; EF, enhancement factor; HSC, human stratum corneum; I_0, the constant rate of iontophoretic drug input into the skin; I_T, the maximum iontophoretic drug input at current removal at time T; J_{ss}, steady-state flux; J(t), flux at time t; k, the rate constant of drug elimination from the central compartment; k_{12}, the rate constant of drug distribution from the central to the peripheral compartment; k_{21}, the rate constant of drug distribution from the peripheral to the central compartment; K_R, the rate constant of drug release from the skin into the systemic circulation (*in vivo*) or into the acceptor phase (*in vitro*); P_{PI}, the zero order mass input into the skin due to passive diffusion post-iontophoresis; S, patch area; T, time of current removal; t', the net time post iontophoresis; t_L, the kinetic lag time of the drug molecules to enter the skin compartment; t_N, the net time of current application; V_{D1}, volume of distribution of the central compartment.

In literature, a number of models have been proposed, focusing on the mechanism involved during iontophoretic transport such as the mobility-pore model (3,4), the ion migration model (5), and the electro-osmosis model (6–8). However, only very few models can describe the *in vitro–in vivo* correlation. Previously, the isolated perfused porcine skin flap (IPPSF) model has been applied successfully to characterize the iontophoretic transport of lidocaine, arbutamine, and luteinizing hormone-releasing factor (LHRH) hormone (9–11). Although this sophisticated model was reported to be superior to predict the *in vivo* situation, the need for special and complex equipment limits its application.

Most commonly, extrapolation methods to predict *in vivo* drug concentrations upon administration by iontophoresis are based on the constant input pharmacokinetics model as proposed by Gibaldi and Perrier (12) that is usually used to analyze the pharmacokinetics of intravenous infusion. In this case, it is assumed that the steady-state flux is achieved very fast. As a result, the drug input into the systemic circulation is assumed to be constant during the entire period of iontophoresis. This model has also been applied to analyze *in vivo* iontophoretic data from several studies as reported by Singh *et al.* (13). However, as the steady-state flux is not always achieved instantaneously, this model might result in an inaccurate estimation.

Furthermore, as the *in vitro–in vivo* correlation has not been examined in great detail, the extrapolations are usually made based on the assumption that the value of the *in vitro* flux is the same as the *in vivo* flux. This assumption may be invalid, as the situation *in vivo* is obviously different from the *in vitro* simulation. Therefore, to achieve a better prediction, this type of correlation should be studied in greater detail, and for a wide array of different compounds. For the *in vivo* situation, a new model based on *in vitro* transport data should be developed that takes into account iontophoretic transport profile during the whole iontophoretic period.

To develop such an *in vitro–in vivo* correlation, this study was aimed to propose a novel compartmental *in vivo* iontophoretic transport model based on the model for *in vitro* iontophoretic transport that has been presented in our previous study. Subsequently, the newly proposed model was applied to fit the published data on the iontophoretic transport of growth hormone-releasing factor (GRF) (14) and R-apomorphine (15) (single-dose iontophoresis) and alniditan (16) (multiple-dose iontophoresis).

THEORY

As mentioned above, during iontophoresis, in most cases, drug input into the systemic circulation varies with time. To address this situation, in this paper time-variant input models are proposed. Furthermore, in order to examine the strength of this novel approach, the constant input models are also reviewed. As pharmacokinetics of several drugs are better described with a multicompartment elimination model, models for drugs with two-compartment elimination kinetics are also derived.

Model of Drugs with One-Compartment Elimination Kinetics

The Constant Input Model

Iontophoretic Period. Assuming that during iontophoresis the steady-state iontophoretic flux is achieved instantaneously, the rate of drug input into plasma is equal to the steady-state flux J_{ss} multiplied by the patch area (S) as written below:

$$\text{Input Rate} = J_{ss}S \tag{1}$$

According to the mass transport scheme as is illustrated in Fig. 1A, for drugs with one-compartment elimination pharmacokinetics, the time-course of the amount of drug in plasma can be described by the following differential equation:

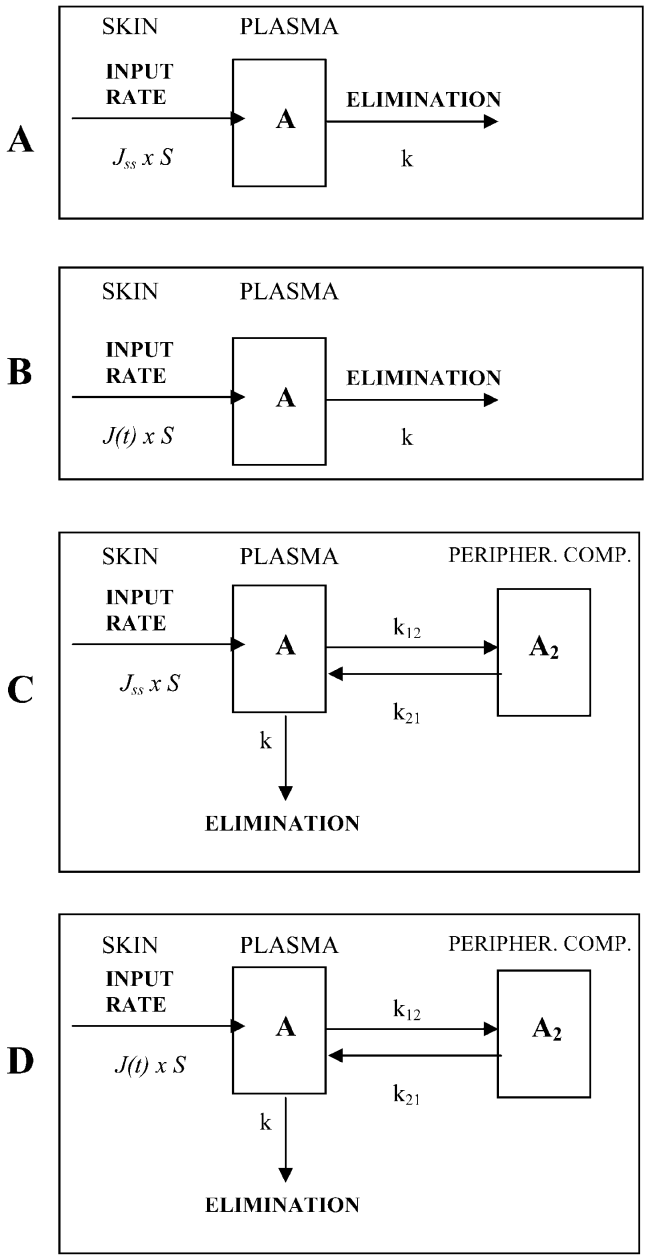

Fig. 1. Scheme of drug transport into the systemic circulation during iontophoresis assuming that the rate of mass input into plasma is a constant J_{ss} (panels A and C) and if the rate of mass input into the skin is determined by the function of flux vs. time [$J(t)$] (panels B and D). Panels A and B illustrate the transport of drug with a one-compartment elimination model, and panels C and D illustrate the transport of drug with a two-compartment elimination model.

$$\frac{dA(t)}{dt} = J_{ss}S - kA(t) \tag{2}$$

in which k is the first-order elimination rate constant of the drug from the systemic circulation and $A(t)$ is the amount of the drug present in plasma at time t. Assuming that there is no drug present in plasma at time zero or $A(0) = 0$, Eq. (2) can be solved as:

$$A(t) = \frac{J_{ss}S}{k}(1 - e^{-kt}) \tag{3}$$

The drug concentration in plasma at time t [$Cp(t)$] can be calculated from:

$$Cp(t) = \frac{A(t)}{V} \tag{4}$$

in which V is the volume of distribution.

Post-iontophoretic Phase. With the constant input model, the transport in the post-iontophoretic period can only be modeled with the assumption that after termination of the current application at time T, there is no further mass input into the systemic circulation. In this case, the mass balance of the drug in plasma can be written as

$$\frac{dA(t)}{dt} = -kA(t') \tag{5}$$

in which

$$t' = t - T \tag{6}$$

Using the initial condition of $A(0) = A_T$, Eq. 5 can be solved as:

$$A(t) = A_T e^{-kt'} \tag{7}$$

in which A_T is the amount of the drug in the systemic at time T. The concentration of the drug in plasma at time t [$Cp(t)$] is again calculated from Eq. (4).

The Time-Variant Input Model

Iontophoretic Period. As already discussed, the flux may change as a function of time. Therefore, the time-course of the amount of drug in plasma (Fig. 1B) can be described by the equation below:

$$\frac{dA(t)}{dt} = J(t)S - kA(t) \tag{8}$$

in which $J(t)$ is the flux function describing the time-dependent drug input into the systemic circulation per cm^2 of the patch area.

Previously (1), we have proposed that during the iontophoretic phase, there is a zero-order drug input from the patch into the skin based on a constant iontophoretic driving force (IDF), whereas the release from the skin into the acceptor phase (*in vitro*) or into the plasma (*in vivo*) is a passive process determined by a first-order skin release rate constant K_R. In that situation, the equation of $J(t)$ is as follows:

$$J(t) = \frac{I_0}{S}(1 - e^{-K_R t_N}) \tag{9}$$

in which I_0 is a zero-order mass transport driven by a constant IDF during current application, S is the area of the patch, and t_N is the net time defined by:

$$t_N = t - t_L \tag{10}$$

in which t_L is the kinetic lag time of the drug to reach the skin compartment. Incorporation of $J(t)$ from Eq. (9) into Eq. (8) yields

$$\frac{dA(t)}{dt} = I_0(1 - e^{-K_R t_N}) - kA(t_N) \tag{11}$$

As no drug is present in plasma at time zero [$A(0) = 0$], Eq. (11) can be solved as follows:

$$A(t) = \frac{I_0(K_R - k + ke^{-K_R t_N})}{k(K_R - k)} - \frac{I_0 K_R}{k(K_R - k)} e^{-kt_N} \tag{12}$$

The concentration of drug in plasma at time t [$Cp(t)$] is calculated from Eq. (4).

Post-iontophoretic Phase. There are two possibilities during the post-iontophoretic period depending on whether the patch is still attached after current removal or whether the patch is removed. If the patch is still attached after current removal at time T, the flux is defined by Eq. (13).

$$J(t) = \frac{P_{PI}}{S}(1 - e^{-K_R t'}) + \frac{K_R}{S} X_T e^{-K_R(t')} \tag{13}$$

in which P_{PI} is the zero-order mass input into the skin due to passive diffusion post iontophoresis and X_T is the amount of drug in the skin when switching off the current at time T. However, if the patch is directly removed after current removal, P_{PI} [thus also the first term in Eq. (13)] is zero, and Eq. (13) can be reduced to Eq. (14).

$$J(t) = \frac{K_R}{S} X_T e^{-K_R(t')} \tag{14}$$

The time-course of the amount of drug in plasma can then be described by the differential equations below:

$$\frac{dA(t)}{dt} = P_{PI}(1 - e^{-K_R t'}) + I_T e^{-K_R t'} - kA(t') \tag{15}$$

or

$$\frac{dA(t)}{dt} = I_T e^{-K_R t'} - kA(t') \tag{16}$$

in which I_T is the maximum iontophoretic drug input into the skin at current removal at time T that is described as follows:

$$I_T = K_R X_T = I_0(1 - e^{-K_R T}) \tag{17}$$

With the initial condition of $A(0) = A_T$, Eqs. (15) and (16) can then respectively be solved as:

$$A(t) = \left(\frac{P_{PI}}{k} e^{kt'} - \frac{P_{PI}}{k - K_R} e^{-(K_R - k)t'} + \frac{I_T}{k - K_R} e^{-(K_R - k)t'} - \frac{P_{PI}K_R - I_T k - k^2 A_T - kA_T K_R}{k(K_R - k)} \right) e^{-kt'} \tag{18}$$

or

$$A(t) = \left(\frac{I_T}{k - K_R} e^{-(K_R - k)t'} + \frac{I_T + A_T(K_R - k)}{K_R - k} \right) e^{-kt'} \tag{19}$$

The concentration of drug in plasma at time t is calculated using Eq. (4).

Models for Drugs with Two-Compartment Elimination Kinetics

The Constant Input Model

Iontophoretic Period. In case the steady-state iontophoretic flux is reached instantaneously (Fig. 1C), the time course of the amount of drug in plasma can be described by the following differential equations:

$$\frac{dA(t)}{dt} = J_{ss}S + k_{21}A_2(t) - k_{12}A(t) - kA(t) \tag{20}$$

$$\frac{dA_2(t)}{dt} = k_{12}A(t) - k_{21}A_2(t) \tag{21}$$

in which $A_2(t)$ is the amount of drug in the peripheral compartment at time t.

With the initial condition $A(0) = 0$ and $A_2(0) = 0$, the differential equations above can be solved for $A(t)$:

$$A(t) = J_{ss}S\left(\frac{(\alpha - k_{21})}{\alpha(\beta - \alpha)}e^{-\alpha}t - \frac{(\beta - k_{21})}{\beta(\beta - \alpha)}e^{-\beta t} + \frac{k_{21}}{\alpha\beta}\right) \tag{22}$$

where α and β are microconstants used during integration/Laplace transformation to solve the differential equations. The micro constants are defined by:

$$\alpha + \beta = k_{12} + k_{21} + k \tag{23}$$

$$\alpha\beta = k_{21}k \tag{24}$$

The concentration of drug at time t [$Cp(t)$] can be calculated as:

$$Cp(t) = \frac{A(t)}{V_P} \tag{25}$$

V_P is the volume of distribution of the central compartment (plasma).

Post-iontophoretic Phase. Similar to the one-compartment model, the post-iontophoretic phase can only be modeled with the assumption that after current termination at time T, there is no drug input into the systemic circulation. In this case, the mass balance for the amount of drug in plasma and in peripheral compartment can be written in the following differential equations:

$$\frac{dA(t)}{dt} = k_{21}A_2(t') - k_{12}A(t') - kA(t') \tag{26}$$

$$\frac{dA_2(t)}{dt} = k_{12}A(t') - k_{21}A_2(t') \tag{27}$$

Using the initial condition of $A(0) = A_T$ and $A_2(0)=A_{2T}$, Eq. (26) together with Eq. (27) can be solved for $A(t)$ as:

$$A(t) = \frac{(k_{21}(A_T + A_{2T}) - \beta A_T)e^{-\beta t'} - (k_{21}(A_T + A_{2T}) - \alpha A_T)e^{-\alpha t'}}{\alpha - \beta} \tag{28}$$

in which A_{2T} is the amount of drug in the peripheral compartment at time T. The concentration of drug in plasma at time t [$Cp(t)$] can be calculated from Eq. (25).

Time-Variant Input Model

Iontophoretic Period. As also discussed with compounds that follow a one-compartment pharmacokinetics model, the iontophoretic flux is often a time course function $J(t)$ rather than a constant J_{ss} (Fig. 3B) as has been defined in our previous paper (1). Therefore, Eq. (23) can be modified into:

$$\frac{dA(t)}{dt} = J(t)S + k_{21}A_2(t) - k_{12}A(t) - kA(t) \tag{29}$$

Analogous to the one-compartment model, after the incorporation of $J(t)$ from Eq. (9), Eq. (29) together with Eq. (21) can be solved by using the initial condition $A(0) = 0$ and $A_2(0) = 0$ to obtain:

$$A(t) = I_0K_R\left(\frac{(k_{21} - \beta)}{\beta(\beta - \alpha)(K_R - \beta)}e^{-\beta t_N} - \frac{(k_{21} - \alpha)}{\alpha(\beta - \alpha)(K_R - \alpha)}e^{-\alpha t_N} + \frac{(K_R - k_{21})}{K_R(K_R - \alpha)(K_R - \beta)}e^{-K_R t_N} + \frac{k_{21}}{\alpha\beta K_R}\right) \tag{30}$$

in which t_N is the net time as defined by Eq. (10). Parameters α and β are the microconstants obtained during integration/transformation as defined in Eqs. (23) and (24). The concentration of drug in plasma at time t [$Cp(t)$] can be calculated using Eq. (25).

Post-iontophoretic Phase. As discussed with the one-compartment model, there are two situations possible, either the patch is still attached or is directly removed after current removal at time T. The flux into the plasma is then defined by Eqs. (13) and (14), respectively. Therefore, the rate of mass transport in plasma can be described by either Eq. (31) or (32).

$$\frac{dA(t)}{dt} = P_{PI}(1 - e^{-K_R t'}) + I_T e^{-K_R t'} + k_{21}A_2(t') - k_{12}A(t') - kA(t') \tag{31}$$

$$\frac{dA(t)}{dt} = I_T e^{-K_R t'} + k_{21}A_2(t') - k_{12}A(t') - kA(t') \tag{32}$$

If the patch is attached, with the initial condition of $A(0) = A_T$ and $A_2(0) = A_{2T}$, Eq. (31) together with Eq. (27) are solved for $A(t)$ to obtain

$$A(t) = P_1 + \frac{(P_2 + P_3)}{\alpha(\alpha - K_R)(\alpha - \beta)}e^{-\alpha t'} + \frac{(P_4 + P_5)}{\beta(\alpha - \beta)(\beta - K_R)}e^{-\beta t'} + \frac{P_{PI}k_{21}}{\alpha\beta} \tag{33}$$

where

$$P_1 = -\frac{(P_{PI} - I_T)(k_{21} - K_R)}{(\alpha - K_R)(\beta - K_R)}e^{-K_R t'} \tag{34}$$

$$P_2 = \alpha P_{PI}K_R + k_{21}A_{2T}\alpha K_R + A_T k_{21}\beta K_R + \alpha I_T k_{21} - A_T k_{21}\alpha^2 \tag{35}$$

$$P_3 = -k_{21}A_{2T}\alpha^2 - P_{PI}K_R k_{21} - A_T\alpha^2 K_R - I_T\alpha^2 + A_T\alpha^3 \tag{36}$$

$$P_4 = -\beta I_T k_{21} - \beta P_{PI}K_R - \beta k_{21}A_{2T}K_R + P_{PI}K_R k_{21} - \beta A_T K_R k_{21} \tag{37}$$

$$P_5 = \beta^2 k_{21}A_{2T} - \beta_3 A_T + K_R\beta^2 A_T + \beta^2 A_T k_{21} + \beta^2 I_T \tag{38}$$

On the other hand, if the patch is directly removed after iontophoresis, the drug amount in plasma can be calculated as:

$$A(t) = \frac{I_T(K_R - k_{21})}{(\alpha - K_R)(\beta - K_R)} e^{-K_R t'} + \frac{R_1}{(\alpha - K_R)(\alpha - \beta)} e^{-\alpha t'} + \frac{R_2}{(\beta - K_R)(\alpha - \beta)} e^{-\beta t'} \quad (39)$$

where

$$R_1 = k_{21}A_{2T}K_R - \alpha A_T K_R + A_T K_R k_{21} + I_T k_{21} - \alpha I_T - \alpha k_{21} A_{2T} + \alpha^2 A_T - \alpha A_T k_{21} \quad (40)$$

$$R_2 = -k_{21}A_{2T}K_R + A_T K_R \beta - A_T K_R k_{21} + I_T \beta - \beta^2 A_T - I_T k_{21} + k_{21}A_{2T}\beta + A_T k_{21}\beta \quad (41)$$

Concentration of drug in plasma at time t [$Cp(t)$] can be derived by using Eq. (25).

METHODS

To test the utility of the proposed *in vivo* models to describe the time course of the drug concentration in plasma upon administration by transdermal iontophoresis, the constant input and the time-variant input models were applied to fit the data of single-dose iontophoresis of GRF 1-44 in hairless guinea pigs (drug amount, 2 mg in 2 g gel; current density, 0.17 mA cm^{-2}; duration iontophoresis, 5 h; patch area, 5 cm^2) (one-compartment pharmacokinetics model) (14) and the iontophoresis data of R-apomorphine in patients with Parkinson disease (drug concentration, 15 mM; current density, 0.25 mA cm^{-2}; duration iontophoresis, 3 h; patch area, 20 cm^2) (two-compartment pharmacokinetics model). Two groups of patients, namely surfactant group and control group, were involved in this study. In surfactant group, the patients received a 3-h pretreatment with the formulation containing laureth-3 ethyloxylene ether, laureth-7 ethyloxylene ether, and sodium sulfosuccinate (0.7/0.3/0.05) prior to application of iontophoresis. In contrast, the patients in the control group directly received the iontophoretic patch without any pretreatment (15). Moreover, as an example of the utility of the time-variant input model to fit a multiple-dose iontophoresis, the data of plasma concentrations of alniditan during a two-dose iontophoresis in eight healthy volunteers (drug amount, 0.5 mg; current density, 0.2 mA cm^{-2}; duration iontophoresis, 0.5 h at t = 0 h and at t = 2 h; patch area, 10 cm^2) (16) were analyzed.

In order to fit the data, the pharmacokinetics parameters of k and V of GRF 1-44 were obtained by fitting the individual plasma concentration data following intravenous infusion provided in the same Ref. (14). For R-apomorphine, the values of the pharmacokinetics parameters of k, k_{12}, k_{21}, and V_P were obtained from Li *et al.* (15). The pharmacokinetics parameters of alniditan (α, β, k_{12}, k_{21}, and V_P) were obtained by fitting the subcutaneous injection simulation of alniditan presented in the same paper (16).

All curve fittings and simulations were performed by using WinNonlin Professional version 4.1 (Pharsight Corporation, Mountain View, CA, USA) (17). The analyses of GRF hormone and R-apomorphine were based on the individual plasma concentration *vs.* time profiles of the drugs. In case of alniditan, as the individual data is not available, the analyses were based on the mean of the plasma concentration *vs.* time profile. Diagnostics of the fitting were based on plots of: the predicted and the observed plasma concentration *vs.* time, the predicted *vs.* the observed plasma concentration, and the weighted residual sum of square *vs.* the predicted plasma concentration. Nelder-Mead algorithm was used during the minimization process with values of the increment for partial derivative, number of predictive values, convergence criterion, iterations, and mode size of 0.001, 1000, 0.0001, 500, and 4, respectively. For all fittings, proportional weighting to the reciprocal of the predicted value was applied.

Moreover, due to the limited number of data points, in order to obtain a better confidence level of the best-fit parameters the fitting of the iontophoretic data to the time-variant input model were typically performed in two steps. The first step was to evaluate whether the parameter t_L should be constrained to a certain value. The second step was the fitting of the same data with the time-variant input model

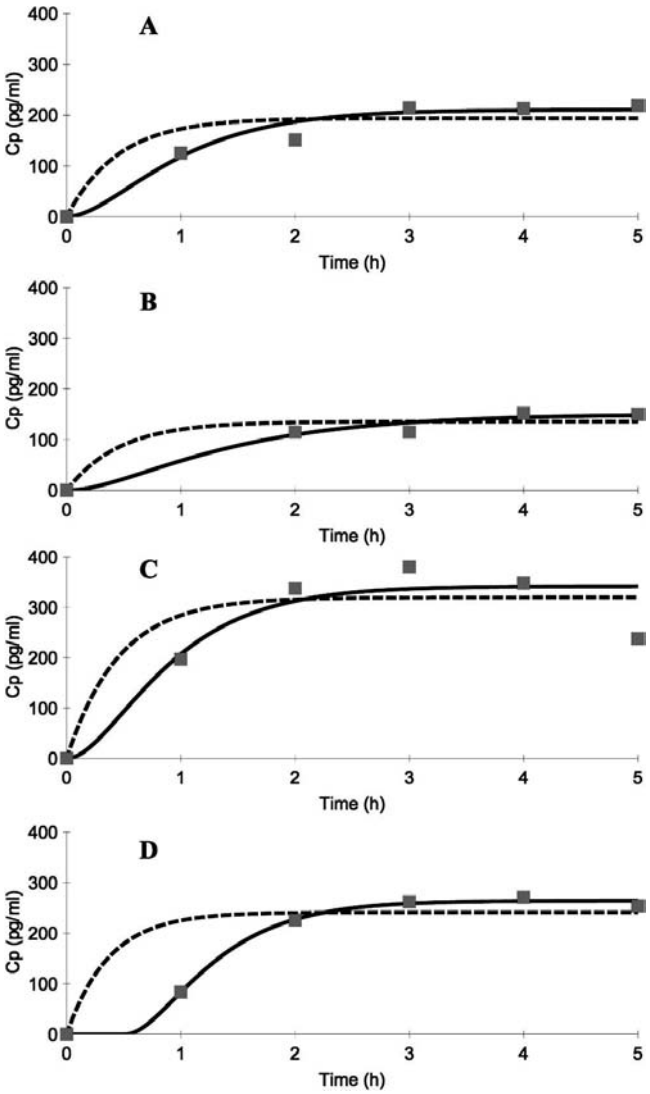

Fig. 2. The observed data (closed square), the prediction based on the constant input model (dashed line), and the prediction based on the time-variant input models (solid line) of plasma concentration *vs.* time profiles of GRF hormone upon transdermal iontophoresis in four hairless guinea pigs. The observed data are obtained from Ref. (14). Terms A, B, C, and D refer to individual animal.

by constraining the value of t_L. For subject D in GRF iontophoresis as well as subjects 3, 7, and 10 in R-apomorphine iontophoresis, the fitting was only performed once, as the good fit and reliable values of the best-fit parameters were already obtained.

Furthermore, based on the best-fit parameters obtained with the time-variant input models, the *in vivo* flux profiles of both GFR and R-apomorphine were simulated. These *in vivo* flux profiles were then compared with the *in vivo* flux profile derived using the deconvolution method. Deconvolution analysis was performed by using Deconvolution Toolbox in WinNonlin Professional v. 4.1.

To estimate the *in vitro–in vivo* transport as well as to find the best *in vitro* system mimicking the *in vivo* transport of R-apomorphine in both surfactant and control/PBS groups, the transport parameters (J_{ss}, K_R, and t_L) from the *in vivo* study were compared to the transport parameters from several *in vitro* studies. The *in vitro* studies consist of: the iontophoretic transport across HSC at room temperature (2), the iontophoretic transport across human stratum corneum (HSC) at 32°C (18), and the iontophoretic transport across dermatomed human skin (DHS) at 32°C (18). In all of these studies, R-apomorphine concentration in the donor phase was 15 mM, current density was 0.5 mA cm^{-2}, duration of iontophoresis was 9 h, and the active diffusion area was 0.64 cm^2.

RESULTS

The Utility of the Models to Fit the Data of Single-Dose Iontophoresis of GRF Hormone

The observed individual profiles of plasma concentration *vs.* time of GRF hormone upon transdermal iontophoresis in four hairless guinea pigs together with the best-fit profiles by the constant input and time-variant input models in combination with a one-compartment model for the elimination kinetics are presented in Fig. 2. The graphs show a clear trend that the time-variant input model better fits to the observed data than the constant input model for all individuals. The typical examples of the visual evaluation based on the predicted *vs.* the observed flux correlation and the weighted residual sum of square vs. the predicted flux, as presented in Fig. 3, confirm that time-variant input model is better to describe the transdermal iontophoresis of GRF *in vivo*.

The final best-fit parameters of J_{ss}, K_R, and t_L for each subject are presented in Table I. Except in subject D (GRF), the values of t_L were negligible (Table I). The parameter J_{pas} was not determined, as the post-iontophoretic period data were not available.

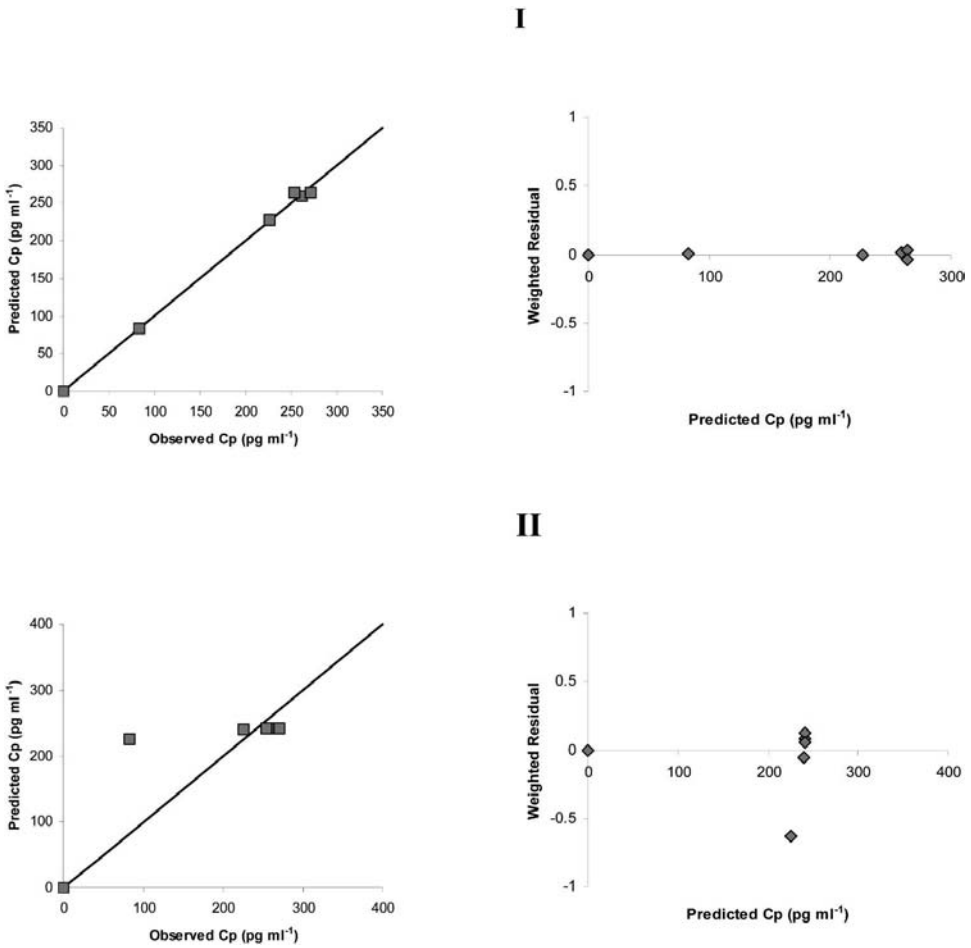

Fig. 3. Typical example of the visual evaluation of the predicted plasma concentration *vs.* the observed plasma concentration (closed square) and the weighted residual vs. the predicted plasma concentration (closed diamond) of GRF hormone of hairless guinea pig D, fitted using the time-variant input model (I) and the constant input model (II).

Table I. The Values of the Best-Fit Parameters Obtained by the Application of the Time-Variant Input Model to the Plasma Concentration *vs.* Time Profiles of GRF, R-Apomorphine, and Alniditan

Drug	Subject ID	J_{ss}[a]		K_R[b]		t_L[c]	
		Mean	%CV	Mean	%CV	Mean	%CV
GRF	A	677.4	6.3	1.6	24.4	0.0	ND
	B	353.4	8.8	0.9	32.6	0.0	ND
	C	1078.5	9.8	1.9	44.5	0.0	ND
	D	796.5	1.9	2.1	20.2	0.5	9.6
R-apomorphine (Surfactant)	1	25.6	9.8	2.4	21.9	0.0	ND
	2	40.9	7.3	2.3	13.7	0.0	ND
	3	34.2	2.2	3.8	10.4	0.0	24.0
	5	32.5	19.3	2.5	44.9	0.0	ND
	6	39.4	7.5	1.9	15.4	0.0	ND
	7	34.3	9.2	3.1	22.4	0.1	8.4
	8	27.3	7.6	3.0	17.7	0.0	ND
R-apomorphine (Control)	10	25.0	8.0	1.5	16.7	0.1	15.9
	11	24.0	12.7	1.4	22.0	0.0	ND
	12	26.1	6.0	3.5	18.7	0.0	ND
	13	27.2	8.1	2.2	15.4	0.0	ND
	14	25.9	4.8	1.9	9.9	0.0	ND
	16	27.9	3.2	1.6	4.7	0.0	ND
Alniditan[d]	Average	68.6	8.4	15.0	52.6	0.0	ND

ND: CV was not determined because the t_L parameter was constrained.
[a] The units of J_{ss} are ng cm^{-2} h^{-1} (GRF) and μg cm^{-2} h^{-1} (R-apomorphine and alniditan).
[b] The unit of K_R is h^{-1}.
[c] The unit of T_L is h.
[d] Parameter J_{pas} of alniditan was estimated as 2.5 μg cm^{-2} h^{-1} with %CV of 19.9.

The Utility of the Models to Fit the Data of Single-Dose Iontophoresis of R-Apomorphine

In Fig. 4, typical examples of the fitting of the plasma concentration of R-apomorphine of both the surfactant pretreatment group (panel A) and the control group (panel B) using the constant input model and the time-variant input model are presented. The superiority of the time-variant input model to describe the transport of R-apomorphine during the iontophoretic period and the post-iontophoresis period is demonstrated while in all cases the constant input model fails to converge the data. Visual evaluation was not performed, as the superiority of the time-variant input model was already obvious. The final best-fit parameters of J_{ss}, K_R, and t_L of all patients are presented in Table I.

The Utility of the Models to Fit the Data of Multiple-Dose Iontophoresis of Alniditan

The utility of the time-variant input model in fitting the plasma concentration of alniditan during a two-dose iontophoresis of alniditan is presented in Fig. 5. Moreover, the figure demonstrates that the time-variant input model is obviously better to describe the plasma concentration *vs.* time profile of alniditan in comparison to the subcutaneous injection simulation as previously used by Jadoul *et al.* (16). The final best-fit parameters of J_{ss}, K_R, and J_{pas} of alniditan are presented in Table I.

The Utility of the Models to Predict *in Vivo* Flux Profiles

The typical examples of the *in vivo* flux *vs.* time profiles are presented in Fig. 6 (GRF) and Fig. 7 (R-apomorphine). The figures demonstrate individual variation in the shape of the curves due to variation in J_{ss}, K_R, and t_L. Moreover, the profiles of flux *vs.* time are comparable to those obtained with the deconvolution method. In addition, the estimated values of J_{ss} obtained using the time-variant input model for GRF and R-apomorphine are very similar to the values estimated with the deconvolution method ($p > 0.05$, paired Student's *t* test) (Table II).

DISCUSSION

Analogous to the *in vitro* models, the proposed *in vivo* time-variant input models introduce in addition to J_{ss} the parameters K_R, J_{pas}, and t_L to describe the drug transport during and post-iontophoresis. Furthermore, particularly in case of iontophoresis of GRF and R-apomorphine, the difference in the shape of the *in vivo* flux profiles between individuals due to the differences in the values of the parameters of J_{ss}, K_R, and t_L (see Table I) is demonstrated.

Time to reach steady-state flux can be estimated based on the values of K_R and t_L as proposed previously (1):

$$99\%\,T_{ss} = t_L - \frac{ln(0.01)}{K_R} \tag{42}$$

in which $99\%\,T_{ss}$ refers to the time to achieve 99% of the steady-state flux. Based on that formula, the average times required to reach the steady-state are approximately 2.3 h in R-apomorphine and 3.3 h in GRF. In the alniditan case, although a steady-state flux can be reached in approximately 0.3 h, this is a relatively significant time period considering the application of current for only 0.5 h. Thus, in all cases there is a significant time delay before steady-state flux is reached, and as a consequence the use of the time-variant input model is superior to the constant input model.

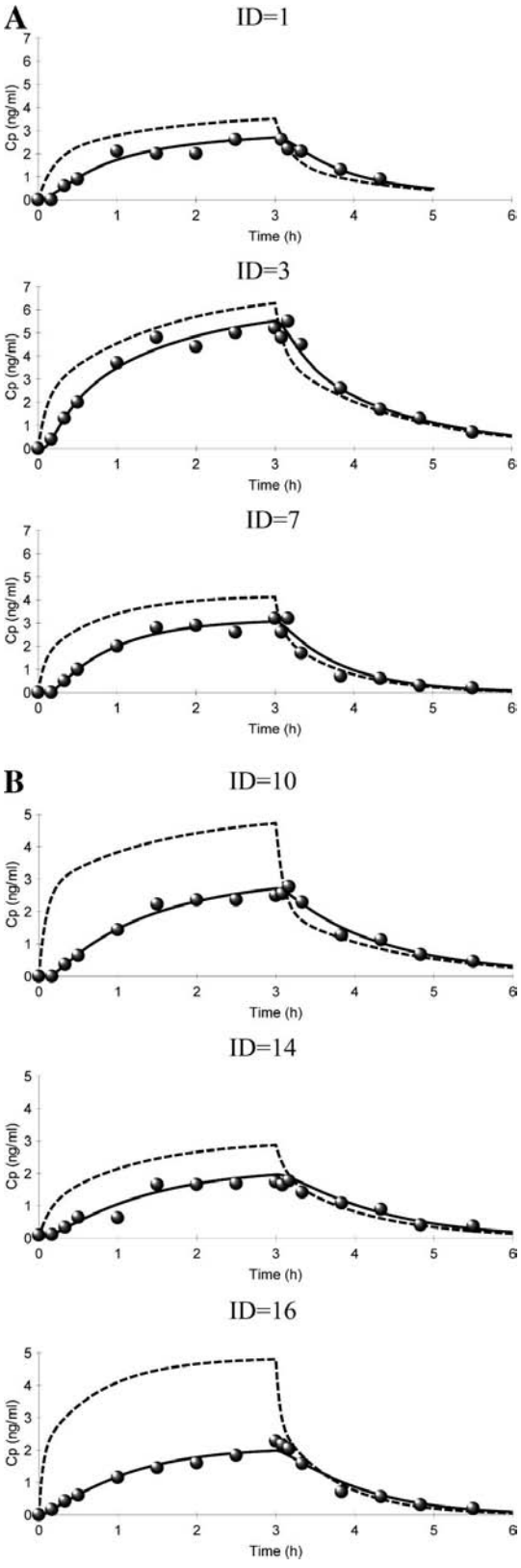

Fig. 4. Typical examples of the observed data (closed circle), the prediction based on the constant input model (dashed line), and the prediction based on the time-variant input models (solid line) of plasma concentration vs. time profiles of R-apomorphine upon transdermal iontophoresis in patients with Parkinson's disease from surfactant pretreatment group (panel A) and control group (panel B). The observed data are obtained from Ref. (15).

In most cases, the values of t_L can be neglected from the model. This is interesting, as we observed previously that in the *in vitro* situation both with R-apomorphine and rotigotine, a statistically significant kinetic lag time was present (1). This is an indication that in the *in vivo* situation, the rate of the drug to enter the skin barrier is somewhat faster compared to the *in vitro* situation. Further investigation is required to explain this interesting phenomenon.

For the first time, elucidation of the *in vivo* flux *vs.* time profile was obtained using an alternative method instead of deconvolution, which has been used previously (15,19). Although the flux levels for GRF and R-apomorphine obtained with both methods are comparable, the prediction on the basis of the compartment model yields a curve that more closely *mimics* the *in vitro* flux profiles that are usually observed (20,21). In contrast, the profiles estimated with the deconvolution method are more scattered with respect to the normal flux *vs.* time profile. It has been discussed previously that the deconvolution method can be subject to numerical instability such as sudden oscillation in the input function. As a result, some noise present in the experimental data can render an error in the earlier estimates that will have a cumulative effect on the subsequent estimates (22).

When comparing the compartment model with the deconvolution method, the advantage of the former is that the parameter J_{ss} can be derived directly based on the best-fit parameters obtained. In contrast, J_{ss} of the profile derived with deconvolution method must be estimated using the diffusion lag time method. Although in cases of GRF and R-apomorphine the values of J_{ss} estimated with both methods are very similar (Table II), the diffusion lag time method possesses some important disadvantages such as the need to exclude some data points and the need to transform the data to allow a linear regression analysis (1). In certain circumstances these disadvantages might be crucial, resulting in an inaccurate estimation of J_{ss}. In addition, as the time-variant input model also estimates other parameters such as K_R, J_{pas}, and t_L, it provides more information regarding the mechanism of the transport during the *in vivo* iontophoresis that is not available with the deconvolution method.

The derivation of the *in vivo* flux as time course profile

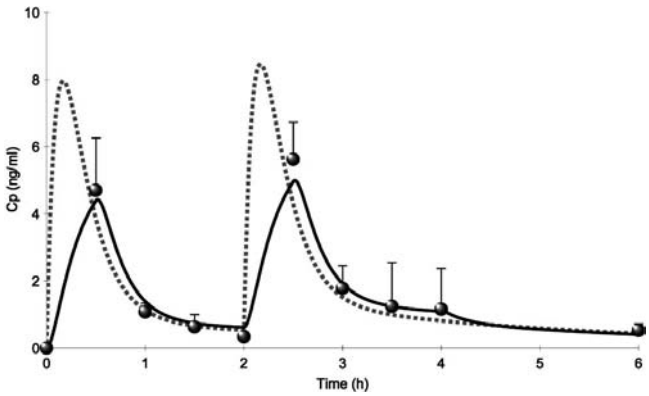

Fig. 5. The observed data (closed circle), the prediction based on the time-variant input model (solid line), and the subcutaneous injection simulation (dashed line) of plasma concentration of alniditan during a two-dose iontophoresis in healthy volunteers. The observed plasma concentration of alniditan and subcutaneous injection simulation are obtained from Ref. (16). Data presented as mean ± SD (n = 8).

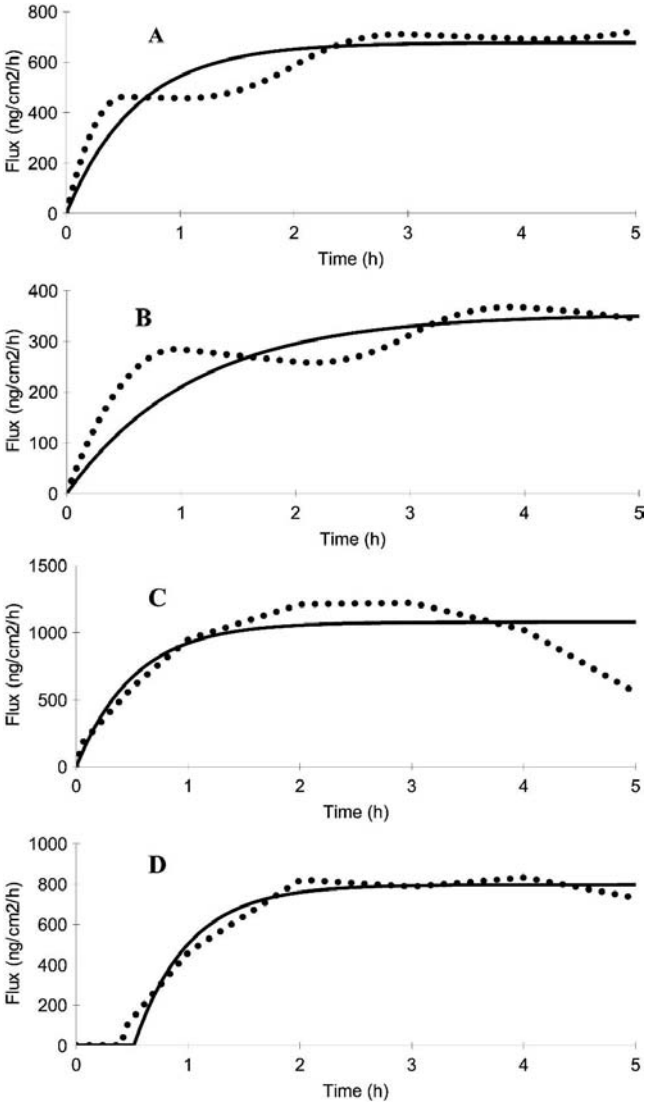

Fig. 6. The prediction of the *in vivo* flux *vs.* time profile of GRF during iontophoresis in four hairless guinea pigs derived based on the time-variant input model (solid line) and the *in vivo* flux *vs.* time profile derived using deconvolution method (dotted line). Terms A, B, C, and D refer to individual animal.

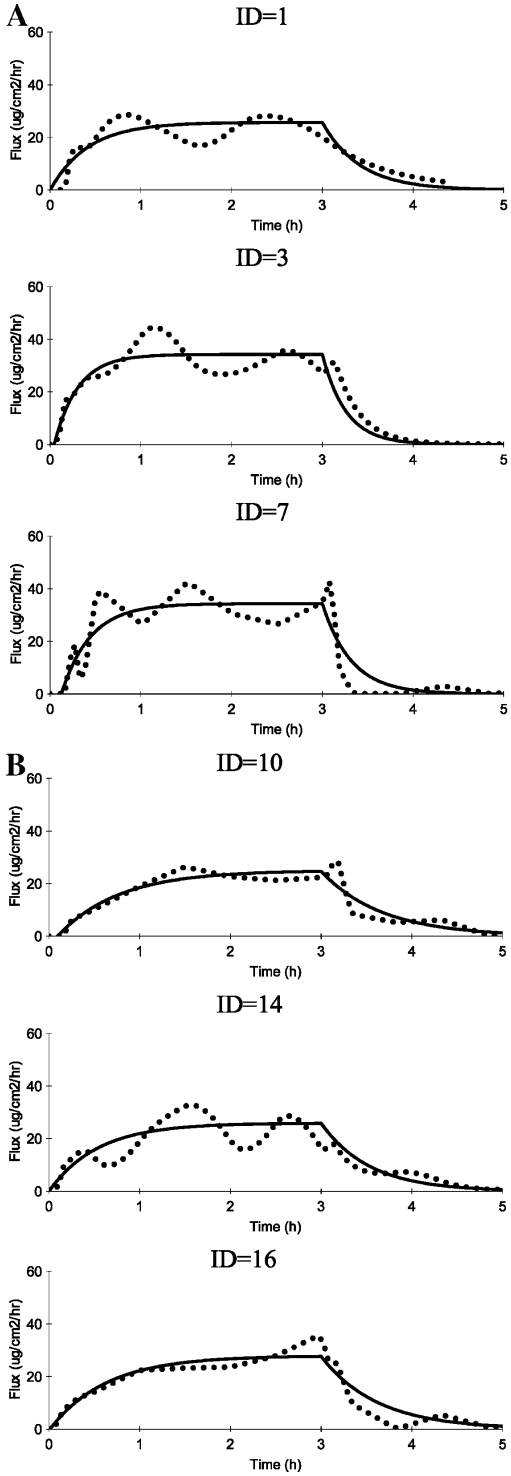

Fig. 7. The typical examples of the prediction of the *in vivo* flux vs. time profile of R-apomorphine during and after iontophoresis in patients with Parkinson disease from surfactant pretreatment group (panel A) and control group (panel B) derived based on the time-variant input model (solid line) in comparison to the *in vivo* flux vs. time profile derived using deconvolution method (dotted line).

based on the fit parameters J_{ss}, K_R, J_{pas}, and t_L offers an important advantage as it allows one to more easily evaluate the efficiency of transport during iontophoresis. The evaluation of the *in vivo* flux profile provides more obvious information than the evaluation of the plasma concentration *vs.* time profile. This is illustrated in the example of R-apomorphine iontophoresis in the control group. Although patient 10 has higher drug concentration in plasma than Patient 14 (Fig. 4B), their *in vivo* flux profiles are similar, even with a significant kinetic lag time for patient 10 (Fig. 7B). Thus, the iontophoretic delivery in patient 14 was more efficient than in patient 10.

Another important benefit of this modeling approach is the possibility to predict and to simulate the *in vivo* profile of multiple-dose iontophoresis in an appropriate way as is illustrated for alniditan. Due to the lack of a specific model, previously the authors presented the data together with a simulation of a subcutaneous injection of alniditan (16). This type of simulation renders an inappropriate prediction of the drug concentration in plasma especially during the iontophoretic period as is clearly demonstrated in Fig. 5. Furthermore, the simulation based on the proposed time-variant input model

Table II. Comparison of the Estimation of J_{ss} During Iontophoresis of GRF and R-Apomorphine Estimated Using the Time-Variant Input Model and the Deconvolution Method

		Time-variant input model		Deconvolution method		
Drug	Unit	Mean	SD	Mean	SD	Significance[a]
GRF	ng cm^{-2} h^{-1}	726.4	300.2	704.9	255.1	$p > 0.05$
R-apomorphine (surfactant)	μg cm^{-2} h^{-1}	33.5	5.7	31.5[b]	3.9[b]	$p > 0.05$
R-apomorphine (control)	μg cm^{-2} h^{-1}	26.0	1.4	24.1[b]	2.1[b]	$p > 0.05$

[a] Based on the paired Student's *t* test.
[b] The values obtained from Ref. (15).

excellently converges to the data during the iontophoretic and post-iontophoretic periods.

The ability to simulate the plasma drug concentration after a multiple dose of iontophoresis is a very important advantage provided by this modeling approach. For example in case of fentanyl, in some cases of severe pain, several iontophoretic dose titration steps are required to achieve the best pain management (23). In this case, the plasma concentration of fentanyl might be simulated using the model whatever fashion is required. Moreover, if the therapeutic window of a drug is known, several types of multiple-dose iontophoretic delivery fashion can be simulated and be adjusted to achieve the most beneficial goal of therapy, particularly the longest duration of action using the same dose of current. This approach might also benefit from the consideration of obtaining the lowest risk of skin irritation due to the application of several shorter periods of current.

Thus, the proposed *in vivo* models with time variant input have shown their utility to describe the profile of plasma concentration as well as to predict the profile of the *in vivo* flux after transdermal iontophoresis. The pharmacokinetics study in the field of transdermal iontophoresis in the future will benefit by this novel approach, which has been demonstrated to be superior to the use of the constant model in all examples shown in this paper.

Furthermore, as we already derived both the *in vitro* and the *in vivo* models of iontophoretic transport that are based on the same assumptions, this is potentially of great value to derive an *in vitro–in vivo* correlation of iontophoretic transport. In order to obtain an ideal correlation, both the *in vitro* and the *in vivo* investigations should have the identical conditions and treatments, particularly the composition of the drug solution in the donor phase/patch and the applied current density.

Although in most cases not all conditions of experimentation *in vitro* are identical to the experimentation *in vivo* and therefore an ideal correlation might not be obtained, several ways of extrapolation may be performed to obtain an approximation of this correlation. Given as an example is the comparison of the *in vivo* R-apomorphine iontophoretic transport to the *in vitro* iontophoretic transport across HSC at room temperature presented in our previous paper (1). The most important difference between this *in vivo* study to the *in vitro* study is the current density used. The current density of 0.5 mA cm^{-2} was used in the *in vitro* study, whereas in the *in vivo* study a current density of 0.25 mA cm^{-2} was applied. As the flux of R-apomorphine was reported to be linearly correlated to the current density (18,21), we could simulate the *in vitro* flux profile from the previous study to the current density of 0.25 mA cm^{-2}. By fitting these simulated data using the *in vitro* compartment model, the best-fit parameters of J_{ss}, K_R, J_{pas}, and t_L were obtained as presented in Table III. The comparison to the *in vivo* parameters is presented in the same table.

Table III. Comparison of the *in Vitro–in Vivo* Best-Fit Parameter of Iontophoretic Transport of R-Apomorphine from Surfactant Pretreatment Group and Control Group Derived Using the *in Vitro* Model and the *in Vivo* Time-Variant Input Model

		J_{ss} (μg cm^{-2} h^{-1})		K_R (h^{-1})		t_L (h)		J_{pas} (μg cm^{-2} h^{-1})	
Group	System	Mean	SD	Mean	SD	Mean	SD	Mean	SD
Surfactant[a]	*In vivo*	33.5	5.7	2.7	0.6	0.0	0.0	ND	ND
	In vitro RT	28.1	3.4	2.6	1.2	0.3[b]	0.1	4.8	0.7
	In vitro 32°C	67.4	13.7	0.9[b]	0.5	0.1	0.1	ND	ND
	In vitro DHS	49.1[b]	5.1	0.4[b]	0.2	0.5[b]	0.3	4.7	3.4
PBS control	*In vivo*	26.0	1.4	2.0	0.8	0.0	0.0	ND	ND
	In vitro RT	13.2[b]	1.2	2.4	0.8	0.4[b]	0.1	2.4	0.6
	In vitro 32°C	28.9	5.3	1.7	1.1	0.1	0.1	ND	ND
	In vitro DHS	34.3	5.1	0.4[b]	0.2	0.7[b]	0.5	1.0	1.5

ND: not determined.
[a] Surfactant pretreatment significantly increased the *in vivo* flux of R-apomorphine, the *in vitro* flux of R-apomorphine across human stratum corneum (HSC) at room temperature (RT), the *in vitro* flux of R-apomorphine across HSC at 32°C, and the *in vitro* flux of R-apomorphine across dermatomed human skin (DHS) at 32°C ($p < 0.05$).
[b] The *in vitro* value is significantly different to the *in vivo* value ($p < 0.05$).

Except with the values of J_{ss} of the control group and the values of t_L in both groups, the *in vivo* values were very similar to the ones obtained *in vitro* at room temperature. Although in the surfactant pretreatment group the *in vivo* value of J_{ss} was similar to the one observed *in vitro*, in the PBS/control group the *in vivo* J_{ss} was more than 2-fold higher than the *in vitro* value. These results indicate that with surfactant pretreatment, the *in vitro* transport at room temperature can mimic the *in vivo* transport, while with the control group it underestimates the *in vivo* transport. However, we also analyzed other *in vitro* data of R-apomorphine transport across HSC and DHS in which the acceptor phase was maintained at 32°C as reported previously (18). The results are also presented in Table III. Interestingly, with the transport across HSC at 32°C, all the *in vitro* parameters (J_{ss}, K_R, and t_L) of the control group are similar to the *in vivo* transport ($p > 0.05$). In contrast for surfactant group, J_{ss} was 2-fold higher than the *in vivo* value ($p < 0.05$), while the K_R was more than 2-fold less than the *in vivo* value ($p < 0.05$). For the transport across DHS at 32°C, the J_{ss} *in vitro* was significantly higher in both the surfactant and the control groups compared to the values *in vivo* ($p < 0.05$). From these results, we can conclude that the diffusion across HSC with the acceptor phase maintained at 32°C might appropriately mimic the *in vivo* transport of R-apomorphine without surfactant pretreatment. Moreover, although the transport across DHS did not appropriately describe the *in vivo* transport of R-apomorphine in both groups, it predicted the enhancement factor (EF) of the surfactant pretreatment to the iontophoretic transport of R-apomorphine very well. In contrast to the transport across HSC at room temperature or at 32°C that respectively predicted the EF values of approximately 2.3 and 2.4, the transport across DHS predicted the EF value of approximately 1.4, which is very close to the enhancement factor *in vivo* (1.3).

Thus, with this *in vitro–in vivo* compartmental modeling approach, we have demonstrated an example of its utility to find the optimum situation of the *in vitro* experimentation that mimics to the *in vivo* condition. Whether the conclusion derived for the transport of R-apomorphine can generally be applied for other compounds, more *in vitro* and *in vivo* investigations based on this modeling approach should be investigated. Although probably not in all situations an *in vivo* iontophoretic transport can be predicted from an *in vitro* experimentation, it should be possible to derive a correction factor that can provide a bridge to fill that gap. With this solution, a prediction of the *in vivo* transport based on the *in vitro* transport will be possible.

In summary, the *in vivo* models based on the compartmental mass transport for iontophoretic transport introducing the use of J_{ss}, K_R, J_{pas}, and t_L parameters have been proposed. The proposed *in vivo* time-variant input model converged to the observed data both for one- and two-compartment pharmacokinetics models in a single- or multiple-dose iontophoresis. In all cases, the use of the time-variant input model is superior to the constant input model and provides some extra information regarding the transport. Finally, the use of these mathematical models is of value in order to derive an *in vitro–in vivo* correlation during transdermal iontophoretic transport and also to search the optimum *in vitro* model that closely mimics an *in vivo* condition as has been demonstrated in case of R-apomorphine transport.

ACKNOWLEDGMENT

This research was supported by QUE Project Batch III 2000–2004, Faculty of Pharmacy, Gadjah Mada University, Yogyakarta, Indonesia.

REFERENCES

1. A. K. Nugroho, O. Della-Pasqua, M. Danhof, and J. A. Bouwstra. Compartmental modeling of transdermal iontophoretic transport: I. *In vitro* model derivation and application. *Pharm. Res.* **21**:1974–1984 (2004).
2. G. L. Li, M. Danhof, P. M. Frederik, and J. A. Bouwstra. Pretreatment with a water-based surfactant formulation affects transdermal iontophoretic delivery of R-apomorphine in vitro. *Pharm. Res.* **20**:653–659 (2003).
3. M. S. Roberts, P. M. Lai, and Y. G. Anissimov. Epidermal iontophoresis: I. Development of the ionic mobility-pore model. *Pharm. Res.* **15**:1569–1578 (1998).
4. P. M. Lai and M. S. Roberts. Epidermal iontophoresis: II. Application of the ionic mobility-pore model to the transport of local anesthetics. *Pharm. Res.* **15**:1579–1588 (1998).
5. J. B. Phipps and J. R. Gyory. Transdermal ion migration. *Adv. Drug Deliv. Rev.* **9**:137–176 (1992).
6. M. J. Pikal. Transport mechanisms in iontophoresis. I. A theoretical model for the effect of electroosmotic flow on flux enhancement in transdermal iontophoresis. *Pharm. Res.* **7**:118–126 (1990).
7. M. J. Pikal and S. Shah. Transport mechanisms in iontophoresis. II. Electroosmotic flow and transference number measurements for hairless mouse skin. *Pharm. Res.* **7**:213–221 (1990).
8. M. J. Pikal and S. Shah. Transport mechanisms in iontophoresis. III. An experimental study of the contributions of electroosmotic flow and permeability change in transport of low and high molecular weight solutes. *Pharm. Res.* **7**:222–229 (1990).
9. J. E. Riviere, B. Sage, and P. L. Williams. Effects of vasoactive drugs on transdermal lidocaine iontophoresis. *J. Pharm. Sci.* **80**: 615–620 (1991).
10. J. E. Riviere, P. L. Williams, R. S. Hillman, and L. M. Mishky. Quantitative prediction of transdermal iontophoretic delivery of arbutamine in humans with the in vitro isolated perfused porcine skin flap. *J. Pharm. Sci.* **81**:504–507 (1992).
11. M. C. Heit, P. L. Williams, F. L. Jayes, S. K. Chang, and J. E. Riviere. Transdermal iontophoretic peptide delivery: in vitro and in vivo studies with luteinizing hormone releasing hormone. *J. Pharm. Sci.* **82**:240–243 (1993).
12. M. Gibaldi and D. Perrier. *Pharmacokinetics*. Marcel Dekker, New York, 1982.
13. P. Singh, M. S. Roberts, and H. I. Maibach. Modelling of plasma levels of drugs following transdermal iontophoresis. *J. Control. Rel.* **33**:293–298 (1995).
14. S. Kumar, H. Char, S. Patel, D. Piemontese, A. W. Malick, K. Iqbal, E. Neugroschel, and C. R. Behl. In vivo transdermal iontophoretic delivery of growth hormone releasing factor GRF (1-44) in hairless guinea pigs. *J. Control. Rel.* **18**:213–220 (1992).
15. G. L. Li. *Transdermal Iontophoretic Delivery of R-Apomorphine for the Treatment of Patients with Parkinson's Disease*. Ph.D. Thesis, Leiden University, Leiden, The Netherlands, 2003.
16. A. Jadoul, J. Mesens, W. Caers, F. de Beukelaar, R. Crabbe, and V. Preat. Transdermal permeation of alniditan by iontophoresis: in vitro optimization and human pharmacokinetic data. *Pharm. Res.* **13**:1348–1353 (1996).
17. WinNonlin Professional v. 4.1. Pharsight Corporation, Mountain View, CA. (2003).
18. G. L. Li, A. Grossklaus, M. Danhof, and J. A. Bouwstra. Iontophoretic R-apomorphine delivery in combination with surfactant pretreatment: in vitro validation studies. *Int. J. Pharm.* **266**:61–68 (2003).
19. R. Van der Geest, T. Van Laar, J. M. Gubbens-Stibbe, H. E.

Bodde, and M. Danhof. Iontophoretic delivery of apomorphine. II: An in vivo study in patients with Parkinson's disease. *Pharm. Res.* **14**:1804–1810 (1997).
20. A. K. Nugroho, G. L. Li, M. Danhof, and J. A. Bouwstra. Transdermal iontophoresis of rotigotine across human stratum corneum in vitro: influence of pH and NaCl concentration. *Pharm. Res.* **21**:844–850 (2004).
21. R. Van der Geest, M. Danhof, and H. E. Bodde. Iontophoretic delivery of apomorphine. I: In vitro optimization and validation. *Pharm. Res.* **14**:1798–1803 (1997).
22. L. Finkelstein and E. R. Carson. *Mathematical Modeling of Dynamic Biological Systems*, 2nd ed. John Wiley & Sons, New York, 1985.
23. S. Grond, L. Radbruch, and K. A. Lehmann. Clinical pharmacokinetics of transdermal opioids: focus on transdermal fentanyl. *Clin. Pharmacokinet.* **38**:59–89 (2000).